

Review

Organic dyes versus adsorption processing

Francisco J. Alguacil and Félix A. López*

¹ National Center for Metallurgical Researcher (CENIM). Spanish National Research Council (CSIC), Avda. Gregorio del Amo 8, 28040 Madrid, Spain; fjalguac@cenim.csic.es

* Correspondence: f.lopez@csic.es; Tel.: +34-915-538-900

Abstract: Even in the first quarter of XXI century, the presence of organic dyes in wastewaters is a normal occurrence in a series of countries, and being these compounds toxics, their removal from these waters is of a necessity. Among the separation technologies, adsorption processing appeared as one of the most widely used to reach this goal. The present work reviewed the most recent approaches (first half of 2021 year) about the use of a variety of adsorbents on the removal of, also, a variety of organic dyes of different nature.

Keywords: organic dyes; adsorption; removal; wastewaters; environment

1. Introduction

Several industries need the use of organic dyes in their respective processing, however, the usefulness of these dyes, either natural or synthetics, present an important odd point: they are toxics for life, thus, their presence in waters, wastewaters, and in general, liquid effluents must be avoided to obey the regulatory discharge laws for these compounds and to decrease the risk of possible contact with humans.

Various technologies seemed to be appropriate for the treatment of organic dyes-bearing waters, but of them, adsorption processing appeared as one of the most used, probably due to its apparent operational simplicity, and to the myriads of potential adsorbents which can be used in this environmental issue.

The importance of these adsorptive methodologies on the removal of organic dyes from waters is reflected in the number of investigations and reviews published along the years. Recently, several reviews about the use of a given type of adsorbents in this role, included silica-based mesoporous materials of the M41S and SBA-n families [1], different types of graphene-based materials [2,3], biochars [4], metal-organic frameworks (MOF) [5,6], various types of polymeric nanofibers [7], metal-doped porous carbon materials [8], and activated carbon fibers [9]

The present work reviews very recent publications (first half of 2021 year) about the use of adsorbents in the removal of organic dyes from waters, in many cases, the investigations are carried out on synthetic solutions, but there are some examples in which adsorbents are used on real waters. Readers must be aware that this review does not include publications about desorption-degradation processing of these toxic chemicals.

2. Results

2.1 Adsorption

Novel magnetic MgFe_2O_4 /crumbled reduced GO nanoparticles, with surface area $35 \text{ m}^2/\text{g}$ and adsorption capacity of near 25 mg/g were used to eliminate methylene blue from solutions [10]. In the investigation several experimental variable were considered: adsorbent dose, dye concentration, pH, rate of agitation, and the change in temperature. The elimination of the dye followed a pseudo second-order reaction:

$$\frac{t}{[MB]_{ad,t}} = \frac{1}{K_{p2}[MB]_{ad,e}^2} + \frac{t}{[MB]_{ad,e}} \quad (1)$$

being characterized by multi-layer formation on the solid surface. In the above equation, $[MB]_{ad,e}$ and $[MB]_{ad,e}$ were the dye concentrations in the adsorbent at the equilibrium and at an elapsed time, K_{p2} was the constant, and t the elapsed time. The values of enthalpy (endothermic process and entropy change (219 J/mol K), indicated a strong interaction between dye molecules and adsorbent surface and an increase of the random arrangement between the organic dye and the solid surface. A 10^{-3} M NaOH solution was used as desorbent. This magnetic separable adsorbent retained 75% of its initial adsorption capacity after four consecutive cycles.

A magnetic metal-organic framework adsorbent ($Fe_3O_4@UiO-66$), based on functionalized magnetic Fe_3O_4 nanoparticles and highly water stable UiO-66, was used to remove methyl orange and methylene blue from aqueous solutions. In the case of methylene blue, the adsorption data fitted well to the linearized Freundlich model:

$$\ln[MB]_{ad,e} = \ln K_F + \frac{1}{n} \ln[MB]_{aq,e} \quad (2)$$

where K_F represented to the constant model, $[MB]_{aq,e}$ was the methylene blue concentration in the solution at the equilibrium, and n_F represented a value which indicates if the process is favorable (n_F greater than 1) or not. The experimental data derived from the adsorption of methyl orange indicated that, the linearized form of the Langmuir isotherm best fitted them:

$$\frac{[MO]_{aq,e}}{[MO]_{ad,e}} = \frac{1}{K_L [MO]_{ad,m}} + \frac{1}{[MO]_{ad,m}} [MO]_{aq,e} \quad (3)$$

in this equation, K_L represented the model constant, and the subscript ad,m represented the maximum dye concentration in the adsorbent. This adsorbent had adsorption uptakes of 244 mg/g and 205 mg/g for methyl orange and methylene blue, respectively.

The adsorption kinetic experiments demonstrated that the adsorption data, for both dyes, well fitted the pseudo-second-order model. The thermodynamic data indicated that the adsorption, of both dyes, onto the adsorbent was spontaneous and presented an endothermic character. To release the dyes loaded onto the adsorbent, water and ethanol under ultrasonic treatment were used. After eight cycles, there was a continuous decrease on the adsorption capacity of both dyes onto the adsorbent.

A super-adsorbent nanocomposite hydrogel adsorbent was prepared by employing vinyl hybrid silica nanoparticles as crosslinking agent [12]. This adsorbent presented a remarkable adsorption capacity (1690 mg/g) towards methylene blue, with a high removal ratio (90%) within 40 min. A 0.1 M HCl solution was used to recover the dye from the loaded adsorbent. After five cycles, there was a continuous decrease, from 899 mg/g to 757 mg/g, in the adsorption capacity.

Two Zr-based metal-organic cages: Zr-MOC-1 (tetrahedral structure) and Zr-MOC-2 (capsule-like cage skeleton) were synthesized under solvothermal conditions [13]. The adsorption performances of Zr-MOCs for organic dyes (methylene blue, crystal violet, methyl orange and orange G) from aqueous solution were reported. The desorption step, using ethanol, was only mentioned in the case of methylene blue.

Using as precursors, the 1D [Mo₃O₁₀]_n²ⁿ⁻ chains and the flexible N,N'-bis(5-methyl-2-pyrazinecarboxamide)-1,2-ethane (bmpae), a 3D metal-organic framework ([Cu(bmpae)0.5(Mo₃O₁₀)(H₂O)]·H₂O) had been hydrothermally synthesized [14]. Its adsorption capacities towards gentian violet and methylene blue were investigated. It was mentioned in the manuscript that acetonitrile was used in the desorption step.

A green route was used to prepare ZnO:NiO nanocomposites, (Z:N), using the Neem leaf extract as a stabilizing agent [15]. Four different samples with three different ZnO:NiO ratios were prepared, namely: 3Z:1N, 1Z:1N, 1Z:3N and 1Z:1N without extract. The different nanocomposites were used for the adsorption of methyl orange from aqueous solutions, being some of the results summarized in Table 1.

Table 1. Dye uptakes onto the various adsorbent tested.

Adsorbent	[MO] _{experimental} , mg/g	[MO] _{model} , mg/g
1Z:1N without extract	4.4	4.4
3Z:1N	5.4	5.9
1Z:1N	5.1	5.8
1Z:3N	12	11

Temperature: 20° C. pH: 4. Time: 2 h

With the adsorbent containing an excess of NiO (1Z:3N), a maximum in methyl orange was reached; it can also be observed how the addition of Neem leaf extract improved the dye uptake. In all the cases, the uptakes derived by the model (eq. (4)) were in accordance with the corresponding experimental values. The adsorption followed the pseudo-first kinetic equation, which in the published manuscript was written as:

$$\log([MO]_{ad,e} - [MO]_{ad,t}) = \log[MO]_{ad,e} - K_{p1}t \tag{4}$$

where K_{p1} represented to the model constant. The procedure followed to reuse the adsorbent was: 0.1 M NaOH (desorption), 0.1 M HNO₃ (neutralizing), washing with water until pH 7 and drying.

An iron-based Fe-BTC MOF, prepared according to an aqueous-based procedure, was used as an adsorbent for the removal of alizarin red S and malachite green from aqueous phases [16]. Optimal adsorption was reached at pH 4, due to the favorable interactions between dyes and the adsorbent. Kinetic investigation concluded that for the two investigated dyes the pseudo-second order model was followed. Accordingly with the Langmuir model, maximum adsorption capacities of 80 mg/g and 177 mg/g were found for alizarin red S and malachite green, respectively. No desorption data were included in the published manuscript.

A surface modification of mesoporous carbon (MC) based on a Diels-Alder [4 + 2] cycloaddition and the multicomponent Radziszewski reactions generated a MC@PIL composite [17]. This adsorbent was used to adsorb Congo red at various experimental conditions: contact time, concentration, pH and temperature. The investigation demonstrated that the dye was adsorbed on the composite within 10 min of contact, whereas the adsorption capacity was near 331 mg/g, which was greater than that found with the pristine mesoporous carbon. In this work, the experimental data were fitted to the non-linear forms of the pseudo-second order kinetic model (eq. 5) and the Langmuir isotherm (eq. 6):

$$[CR]_{ad,t} = \frac{K_{p2} [CR]_{ad,e}^2 t}{1 + K_{p2} [CR]_{ad,e} t} \quad (5)$$

$$[CR]_{ad,e} = [CR]_{ad,m} \frac{K_L [CR]_{aq,e}}{1 + K_L [CR]_{aq,e}} \quad (6)$$

where [CR] represented the Congo red concentration. Desorption was carried out, as literally written in the published article “...contained a certain proportion of water/ethanol (45%) and a few drops of 1 M NaOH solution during one hour”. Under continuous use, and after three cycles, the desorption rate decreased from 87% to 81%, and thus, the adsorption capacity decreased from 331 mg/g until near 200 mg/g.

The solvothermal self-assembly between Cd^{2+} and a hexacarboxylic acid created a porous material formulae as $[(CH_3)_2NH_2]_6[Cd_3(L)_2] \cdot 5DMF \cdot 3H_2O$, where H6L responded to 3,4-di(3,5-dicarboxyphenyl)phthalic acid, which adsorbed selectively cationic dyes respect neutral or anionic compounds [18]. The investigation was based on the adsorption of azure A+ and methylene blue+. with adsorption capacities of 698 mg/g (azure A+) and 573 mg/g (methylene blue +). Since acetonitrile can not desorb the dye, desorption was performed using a NaCl-acetonitrile solution, the mission of Na^+ ions was to displace the dye cation to conserve the stability of the adsorbent skeleton, and charge balance. After five cycles, both adsorption and desorption capacities slightly, but continuously, decreased.

A carboxyl-functionalized covalent organic framework (TpPa-COOH) was synthesized under environmental pressure, and the adsorptive properties were investigated using eosin B (anionic dye) and the cationic dyes methylene blue and safranin T [19]. TpPa-COOH showed a selective adsorption effect on the two cationic dyes. In these two cases, the adsorption isotherm responded to the Langmuir, with maximum capacities of 1135 mg/g (safranin T) and 410 mg/g (methylene blue). The desorption step was only investigated in the case of safranin T, the step was carried out with THF and 1 M HCl, further, the lean adsorbent was washed with ethanol and dried under vacuum, at 60° C, during twelve hours. After three cycles, the removal efficiency decreased from 99% to 95%

The superparamagnetic Mn-metal organic framework (MOF) with core-shell nanostructures synthesized by in situ way was synthesized as a magnetic adsorbent for malachite green removal from aqueous solution [20]. Three variables were investigated: pH, contact time, and agitation speed. The results show that $CoFe_2O_4@Mn-MOF$ core-shell removes about 98% of the dye from water medium. This reference seemed to be a rare exception, considering many of the published adsorption studies, in which the agitation speed was considered an experimental variable to investigate. The effect of this variable on malachite green adsorption was investigated in the 100-400 min^{-1} range, the results showed that maximum adsorption (99%) was reached at 200 min^{-1} , this result was attributable to the decrease of the film boundary layer which wrapped particles, and thus adsorption increased. No desorption data were included in the investigation.

It was reported [21], the preparation of carboxylic acid-modified polysilsesquioxane aerogels via a straightforward acid-base catalyzed sol-gel approach by using MTMS, and the novel and stable, 5-(trimethoxysilyl)pentanoic acid. Besides the adsorption of heavy metals (zinc(II) and copper(II)), the adsorbent was used in the removal of methylene blue and rhodamine B. Experimental data fitted well with Langmuir isotherm, being the maximum adsorption capacities 154 mg/g (rhodamine B) and 106 mg/g (methylene blue).

An increasing content of carboxylic acid groups influenced the morphology, specific surface area and adsorption behavior of the synthesized aerogels. Desorption was investigated in the case of methylene blue, loaded dye onto the adsorbent was desorbed using HCl solutions of pH 1-2 for 24 hours. Under continuous use, the adsorption

efficiency was near 92% for the three firsts cycles, but decreased from the fourth cycle, whereas desorption maintained an 87% for the fourth and fifth cycles. These carboxylic acid-modified aerogels only remove positively charged molecules from mixed dye solutions.

Being a natural, low-cost and eco-friendly material, naturally occurring alumina particles were used as an adsorbent for the removal of eriochrome black T (anionic dye) from an aqueous environment [22]. The adsorption process can be controlled by electrostatic attractions, and the experimental data were well described by the pseudo-second order kinetic model, and the adsorption isotherms fitted well with the Langmuir isotherm. The maximum adsorption capacity was found to be 45 mg/g, which corresponded to a 71% of dye removal. The adsorption was endothermic and spontaneous.

The desorption procedure and reconditioning of the adsorbent for its reuse followed several steps: i) desorption with 0.1 M NaOH solution during three hours, further ii) washing with HCl and water, and iii) drying at 60° C for 24 hours. Over four consecutive cycles, adsorption decreased in a continuous form from 43 mg/g to near 36 mg/g, at the same time, the desorption efficiency decreased from 71% to 60% after the fourth cycle.

ZnO–CdWO₄ nanoparticles have been synthesized by a green method with lemon leaf extract to favorably anchor functional groups on their surface [23]. The prepared nanoparticles were used as adsorbent of Congo red. The adsorption process was found to be exothermic and spontaneous, and followed the Freundlich isotherm model. The Boyd plot had been used as a confirmatory tool to fit the adsorption kinetics data along with intraparticle diffusion and pseudo-second-order models. No desorption data were included in the work.

Hollow polydopamine microcapsules (H-PDA-MCs), synthesized by an oxidation self-polymerization of dopamine using iron trioxide (Fe₂O₃) nanocube, were used to adsorb cationic dyes as methylene blue [24]. The results showed that at near 25° C, the maximum adsorption capacity was 192 mg/g, being the equilibrium reached within one hour. The data fitted to the pseudo-second-order kinetic model, whereas also fitted to the Langmuir model and Temkin isotherm:

$$[MB]_{ad,e} = B_1 \ln K_T + B_1 \ln [MB]_{aq,e} \quad (7)$$

where B_1 represented the Temkin constant associated to adsorption heat and K_T was the equilibrium binding constant. The increase of the temperature increased the dye uptake onto the adsorbent (Table 2), and thus, the adsorption was an endothermic and spontaneous process. In this system, desorption was performed with a 1 M HCl solution and sonication for 60 min, and after a post-treatment, the adsorbent was reused.

In the next reference [25], and against it was written in the published Abstract, the investigation was not carried out on an industrial wastewater, but on a synthetic solution of water containing the organic dye. Metal organic framework Fe-MIL-88NH₂, with composition (Fe₃O(OH₂)₃Cl(NH₂-BDC)_{3.9}.5H₂O), were used to remove Congo red (5-60 mg/L) from water. Temkin adsorption isotherm model and pseudo-second kinetic model best fitted to the experimental data. The removal of the dye from the water responded to a chemical adsorption process. This adsorbent presented a certain grade of selectivity with respect Congo red and against methyl orange and methylene blue. Desorption of loaded Congo red was done using ethanol, and after four cycles, the removal efficiency was fixed above 83%.

Table 2. Effect of temperature on the theoretical maximum adsorption capacity.

Temperature, °C	[MB] _{ad, m} , mg/g
-----------------	------------------------------

20	228
25	233
30	237

MB: methylene blue

The mixture of chitosan beads crosslinked with glutaraldehyde was used to investigate the adsorption of reactive blue 4 from an aqueous solution [26]. The response surface methodology was applied to evaluate the concentration of chitosan, glutaraldehyde and sodium hydroxide on the swelling degree in the adsorbent. The design with r^2 of 0.8634, allowed to the best concentrations as chitosan (3.3% w/v), glutaraldehyde (1.7% v/v) and NaOH (1.3 M), however, for practical purposes aiming to decrease the viscosity and facilitate the formation of the beads; the real chitosan concentration used in the experiments was of 3.0%. In the case of the dye adsorption, the best conditions ($r^2= 0.8280$) were pH 2, adsorbent dosage 0.6 g and initial dye concentration 5 mg/L. The adsorption process was controlled mainly by chemisorption interactions, and responded well to the Elovich model:

$$[RB4]_{ad,e} = \frac{1}{\beta} \ln \alpha \beta + \frac{1}{\beta} \ln t \quad (8)$$

and Freundlich isotherm. In eq. (8), α represented the initial adsorption rate, and β the desorption constant, this last parameter also corresponded to the extent of surface coverage and activation energy for a chemisorption mechanism. No desorption data were included in the investigation.

The adsorption of methyl orange and fluorescein sodium was investigated using three 3D coordination polymers A: (CPs), $[Cd(L)(bifu)]_n$, B: $[Zn(L)(bimb)_{0.5}]_n$ and C: $[Ni(L)(bifu)](H_2O)_4$, being H₂L: 4,4'-(phenylazanediy1)dibenzoic acid, bifu: 2,7-bis(1-imidazolyl)fluorene, and bimb: 1,4-bis(imidazol-1-yl) [27]. The 3D network structures were different since A crystallized in a monoclinic space group P21/n, B crystallized in a orthorhombic space group Pbca and C crystallized in a triclinic space group P-1. The adsorbents were not suitable for the adsorption of methylene blue and rhodamine B. No desorption data were included in the work.

Hierarchical microspheres of ZnOHF was produced using DL-alanine as the structure-directing agent [28]. These microspheres were formed by numerous nanotubes and were used in the adsorption of organic dyes, though the adsorption of cationic dyes was favored with respect to neutral or anionic dyes. Adsorption data fitted to the Langmuir isotherm and pseudo-second-order kinetic model. Maximum adsorption capacity of the microspheres was 140 mg/g for malachite green at 25° C, in an endothermic and spontaneous physical adsorption process. After five cycles, adsorption decreased from 100% to 75%, though it was not indicated if the dye was desorbed, or the adsorbent was used without desorption.

Mesoporous silica derived from iron ore tailings was synthesized [29], and used in the adsorption of methylene blue. The removal of the dye (pH 10) responded to the Langmuir isotherm and to the pseudo-second order equation, and thus to a monolayer adsorption, being the adsorption capacity of 192 mg/g. The desorption step was not considered here.

Methylene blue and basic violet 16 dyes were remove from aqueous solution using sulfonated poly(ether ether ketone) (sPEEK) [30]. Kinetic experiments revealed that in the case of both dyes, data were well-fitted by the pseudo-second order kinetic model, whereas. the required times to achieve equilibrium were determined as 40 and 20 min for methylene blue and basic violet 16, respectively. Maximum adsorptions occurred at pH of 3-6 (methylene blue) and 3 (basic violet 16). The adsorptions responded to the Langmuir

model, and the maximum adsorption capacities were found to be 98 mg/g (methylene blue), and 182 mg/g (basic violet 16). In the case of methylene blue, the adsorption process presented an endothermic and spontaneous character. In the case of methylene blue, desorption was done using 3 M nitric acid/ethanol (30/70 % v/v) mixtures for 20 minutes, and recycling experiments, on methylene blue, showed that the adsorption efficiency, after five cycles, decreased from 99.6% to 99.2%, whereas low desorption percentage values of basic violet 16V16 indicated that this adsorbent may be used for immobilizing the dye.

Magnetic chitosan hydrogel beads, based on chitosan biopolymer, magnetic graphene oxide nanoparticles (GO/Fe₃O₄), and isophthaloyl chloride, were prepared and used in the removal of cationic and anionic dyes from aqueous solution [31]. Experimental results showed that data were best fitted to the pseudo-second order kinetic model and non-linear Langmuir isotherm. The maximum adsorption capacities of methylene blue and eriochrome black T were 289 (pH 8-10) and 292 pH 3) mg/g, respectively. The removal of the dyes from the solution was associated to an endothermic, spontaneous and favorable process, since the R_L values derived from:

$$R_L = \frac{1}{1 + K_L [\text{dye}]_{\text{aq},0}} \quad (9)$$

where 0.012 (methylene blue) and 0.010 (eriochrome black T). In the above equation, K_L represented to the Langmuir constant estimated by the corresponding fit, and $[\text{dye}]_{\text{aq},0}$ was the initial dye concentration in the aqueous solution. Dyes uptake was attributed to the electrostatic interactions of the dyes with the primary amine, hydroxyl and carboxyl groups of the adsorbent beads. Desorption was performed using HCl (pH 3) in the case of methylene blue, or NaOH (pH 9) in the case of eriochrome black T. The adsorption-desorption properties were well maintained up to four cycles, but from the fifth cycle began to decrease.

A natural adsorbent of graham flour was selected as an adsorbent to remove cationic crystal violet from water [32]. The effective pH range for dye adsorption was neutral pH region, following the Langmuir isotherm, and being the maximum adsorption capacity of 162 mg/g. The polymeric GF adsorbent was selective respect to crystal violet from synthetic polluted sample even in the presence of high concentration of diverse competing ions. The adsorbed can be desorbed with ethanol, being observed a continuous decrease in its capacity up to seventh cycles.

The next reference deals with the encapsulation of methylene blue on the polymeric natural carbohydrate of turmeric powder adsorbent [33]. Maximum dye removal of 99.5% was obtained at pH 7. In the acidic pH region, the positively charged protonated adsorbent did not favor the adsorption of positively charged protonated methylene blue due to electrostatic repulsion. In the neutral pH area, the remove of the dye from the solution was explained by electrostatic attraction and complexation of the dye with the adsorbent. The adsorption data were fitted to the Langmuir isotherm, with a maximum adsorption capacity of 157 mg/g. Ethanol can be used to desorb the dye from the adsorbent; its original capacities were reduced up to seventh cycles..

A series of enantiomorphous Pb-based metal-organic coordination polymers, i.e., [Pb((R,R)-TBA)(H₂O)]·1.7H₂O (R1) and [Pb((S,S)-TBA)(H₂O)]·1.7H₂O (S1) (TBA= 1,3,5-triazin-2(1H)-one-4,6-bis(alanyl)), had been synthesized through solvothermal reactions [34]. Compounds R1 and S1 crystallizing in the chiral space group, P212121, reveal infinite unidimensional (1D) chain structures. These complexes showed a selective adsorption of anionic organic dyes (e.g. Congo red) via a host-guest hydrogen bonding interaction, electrostatic attraction, π - π stacking between the Pb complex and the organic dye. Dye uptake reached 140 mg/g and followed the pseudo-second order kinetic model. No desorption data included in the work.

Sulfonic acid-functionalized carbon nanotubes (CNT-FA-SA) composite was synthesized by Diels-Alder (DA) chemistry and electrophilic substitution reaction [35], and the adsorption of methylene blue onto CNT-FA-SA was investigated. The loading capacity, in an exothermic adsorption process, increased with the increase of the pH from 2 to 12. The non-linear fitting of the data to Freundlich or Langmuir isotherm models estimated that the maximum adsorption capacity of monolayer was 1584 mg/g. The adsorption kinetic responded to the non-linear form of the pseudo-second order equation. The data indicated that the adsorption process was related to chemisorption and physical adsorption simultaneously, and that the adsorption occurred on a heterogeneous multilayer surface. No desorption data were included in the manuscript.

Methyl blue was removed from water by ordered mesoporous silica SBA-15 [36]. The adsorbent was synthesized by silica functionalization with β -cyclodextrin via amide linkage. The adsorption properties of this adsorbent were investigated under several variables: contact time, pH, ionic strength, temperature and salt. The maximum dye adsorption capacity was of 1791 mg/g, being the adsorption following both the non-linear forms of the Langmuir and Freundlich isotherms, thus, the dye uptake was attributed both to homogeneous and heterogeneous mechanisms. The organic dye uptake presented a slight decrease in the 2-5 pH range, and an important decrease from neutral and alkaline values. The adsorption capacity towards the dye was explained in terms of the tailored host-guest interaction between β -cyclodextrin cavity and aromatic moiety of the dye, and in combination with the electrostatic attraction between amine groups and sulfonated group presented in the organic dye. Ethanol was used to desorb the dye, and there was a continuous decrease in the uptake capacity up to six cycles.

A trichlorotriazine-derived calix[4]arene and 1,3,5-tris(4-aminophenyl) benzene were crosslinked to produce a calix[4]arene crosslinked polymer with adsorptive properties towards cationic dyes from water [37]. This polymer showed removal efficiency over 99.6% and 99.4% for methylene blue and toluidine blue within 5 min, respectively, showing Table 3 some of the equilibrium capacities obtained with this adsorbent. In the case of methylene blue and toluidine B, the adsorption followed the pseudo-second order model and the Langmuir isotherm. Maximum equilibrium adsorption capacities for methylene blue and toluidine blue were 1807 and 2161 mg/g, respectively. These results were attributable to electrostatic interactions, π - π interactions, and hydrogen bonding between the polymer and the organic dyes. In column experiments, the removal of the above dyes was of 99%, except in the case of sodium fluorescein which reached 80%.

Table 3. Equilibrium capacities of the adsorbent.

Dye	[Dye] _{ad,e} , mg/g	Dye	[Dye] _{ad,e} , mg/g
methylene blue	252	crystal violet	1.6
toluidine B	226	rhodamine B	2.0
methyl orange	47	sodium fluorescein	4.2

pH 10. Time: 30 min

Desorption was investigated in column operation, and using methanol as desorbent; after five cycles, the removal efficiency was greater than 95%.

The ternary Cu/Cu₂O/C composite presenting anionic dyes adsorption capacities was synthesized by a solvent-free method [38]. The maximum monolayer adsorption capacity of Cu/Cu₂O/C for methyl orange and acid blue 93 was 1409 and 5385 mg/g, respectively. Besides, the Cu/Cu₂O/C composite can selectively adsorb anionic dyes (methyl orange and acid blue 93) from a mixture of different dyes. The increase in the adsorbent dosage allowed to achieve the equilibrium at shorter reaction times, whereas maximum uptakes (99%) were reached at pH 4.7, decreasing this value until 50% at pH 11. The various experimental data indicated that the adsorption process followed the Langmuir isotherm and the pseudo-second-order kinetic model, whereas the removal of both dyes from water was spontaneous and exothermic in nature. Based on the experimental results and the characterization of the composite, it can conclude that the physical and chemical synergism effect existed in the adsorption process, and chemisorption was the main rate limiting step. Desorption was achieved using hot water (90° C) and ethanol, and after three cycles, the removal rate decreased from 99% to 75%; this decrease was attributable to i) the partial oxidation of Cu₂O or Cu on the surface of the composite, and ii) the desorption was not complete.

A boron-doped mesoporous carbon materials was generated from F127, as the soft template, and phenolic resin and triisopropyl borate were selected as carbon and boron containing precursors [39]. The prepared material had been used in the adsorption of crystal violet and Congo red dyes. In both cases, the experimental data fitted the Langmuir isotherm and the pseudo-second kinetic equation, with dyes uptakes of 385 mg/g (crystal violet) or 323 mg/g (Congo red). After five rounds of circulation, the removal rate decreased from 79% to 63% (Congo red) or 94% to 80% (crystal violet), this decrease may be caused by the disappearance or weakening of the vacancy sites on the adsorbent in the desorption process. It was not clearly mentioned, in the published manuscript, how the desorption procedure was carried out.

A hexatungstate derivative, [Ni₂(L)₃]₂[W₆O₁₉]·2H₂O, being HL: 2-acetylpyrazine-N(4)-methyl thiosemicarbazone, had been synthesized, characterized and used in the adsorption of methylene blue, gentian violet and fuchsin basic [40], with removal efficiencies of 99%, 94% and 94%, respectively. The different reactivity over the various dyes was caused by the electrostatic interactions between the dyes and the [W₆O₁₉]²⁻ molecules. Methylene blue uptake onto the adsorbent followed the pseudo-second-order kinetic equation. After five cycles of adsorption-desorption, the capacity decreased from, 99% to 82%, being this decrease attributable to the loss of adsorbent during each washing step.

The adsorption performance of delaminated Ti₃C₂-MXenes towards six different organic dyes in aquatic media at different pH levels and ionic strengths was investigated [41]. The ability of this adsorbent to remove the dyes was based on the electrostatic interactions between the ionizable functional groups of MXenes and dyes. The pH had a different influence in the dye adsorption, in the case of methylene blue, the adsorption of this dyer increased with the pH value from 2 to 10, methyl orange presented an increase in its adsorption from pH 2 to 4, with a further stabilization until pH 10, the removal of Congo red was stable in the 2-10 pH range and then decreased until pH 12, methyl red was adsorbed in the range 2-4 with a sharply decrease up to pH 10 (negligible adsorption), whereas in the case of orange G, a 60% adsorption rate was achieved at pH 2, and near zero at pH 4. In water, methyl red adsorption was attributable to the intraparticle diffusion model:

$$[MR]_{ad,t} = K_p t^{0.5} + [MR]_{ad,t=0} \quad (10)$$

where K_p represented the rate constant; in all the other dyes, the fitting of the results was not clear. No desorption data were included in the work.

Rice husk ash can be used as a sustainable source of silica for producing high valuable subproducts. This product served as precursor of mesostructural graphene oxide, and used to adsorb methylene blue from solutions via oxygen functional groups presented in the adsorbent [42]. The adsorption capacity depended on the gelation pH, grapheme oxide content, adsorbent dosage, and initial dye concentration. The highest adsorption capacity was 633 mg/g, and the data fitted to the Freundlich or Langmuir models depending of the type of adsorbent material used in the investigation. In all the cases, the data fitted to the pseudo-second order kinetic model. Desorption information was not included in the manuscript.

Combustion and gel calcination operations were used to prepare magnetic $\text{Zn}_{0.3}\text{Cu}_{0.7}\text{Fe}_2\text{O}_4$ nanoparticles (50-50 nm) and used to adsorb reactive red 2BF [43]. Experimental data, using dye concentrations in the 100-400 mg/L range, fitted to the non-linear pseudo-second-order kinetics, whereas Temkin isotherm explained the experimental loading equilibrium data, thus, adsorption was due to a monolayer-multilayer hybrid adsorption mechanism. The dye adsorption capacity reached 135 mg/g, though was pH-dependant, with maximum adsorption in the pH range 1-3, and a progressive decay to near zero adsorption at pH 11. Desorption can be carried out under alkaline conditions, however, a continuous decrease in adsorption rate, from 100% to near 80%, was observed after ten cycles. This decrease was attributable to that nanoparticles agglomerated and the adsorption sites gradually decreased, and also to the gradual loss of the adsorbent material.

HKUST-1/cellulose/chitosan aerogel composite, with hierarchical pores, was investigated to remove methylene blue [44]. With a high adsorption capacity (526 mg/g), the removal of the dye increased from pH 3 to 7, levels off until pH 8 and then decreased from pH 9 to 11. It was determined that the adsorption occurred through H-bond interactions between oxygen and nitrogen atoms in the composite aerogel and nitrogen atoms from the organic dye. The adsorption fitted to the pseudo-first and pseudo-second order models, and thus, the adsorption was due to a synergistic effect of chemical and physical mechanisms. Desorption was investigated using ethanol and water under lyophilization. After five cycles, the adsorption capacity decreased from 162 mg/g to 153 mg/g.

The adsorption behavior of different adsorbents has been studied by various research works. But few studies have compared linear and non-linear isotherm and kinetic models alongside phenomenological coefficients. The effect of activated carbon black on methylene blue adsorption behavior of alginate was examined [45]. A low-cost and green adsorbent was fabricated to can easily be detached from water. The results were well fitted with non-linear pseudo-second-order and linear Langmuir models. Intraparticle diffusion model and phenomenological coefficients represented control of adsorption by film diffusion and its limiting by pore diffusion. No desorption data were included in the work.

Highly dispersed graphene nanosheets were directly integrated into polyurethane sponge, the resulting material was used as adsorbent towards methylene blue, ethidium bromide and eosin Y [46]. The dyes uptake followed the Langmuir isotherm model, which was an evidence of a strong monolayer chemisorption; in the three cases, the adsorption process was spontaneous and exothermic, also, dyes uptake fitted to the pseudo-second-order kinetic model. In the case of the cationic dyes, the adsorption increased with the increase of the pH, e.g. maximum adsorption capacity at pH 10 within methylene blue and ethidium bromide, whereas anionic dyes followed the opposite tendency, e.g. pH 3 for eosin Y. Again, desorption data were absent in the work.

An aerogel formed by graphene-polydopamine-bovine serum albumin, to which biopolymers were added, was used in the removal of organic dyes (methylene blue and Evans blue), toxic metals (Cr(VI) and Pb(II)) and organic solvents (n-hexane, n-heptane, and toluene) [47]. In the case of both organic dyes, the adsorption capacity increased when the pH value increased from 2 to 8. Desorption was only investigated in the case of

methylene blue, using ethanol at pH 2 during 24 hours. After three cycles, the removal efficiency for methylene blue decreased by 2-20% (depending of the dye concentration). The system was used in a continuous form using a flow-through filtration system..

A polyurethane/polyaniline material that can be used as an adsorbent for azo dyes from aqueous solutions was developed [48]. This adsorbent was generated by incorporating polyaniline into the surface of a macroporous polyurethane foam by a chemical polymerization methodology. The adsorption capacity of the material was evaluated against the removal of methyl orange at various pH values, contact time and initial concentration. The adsorption reached equilibrium after 30 h, following the Elovich and the intraparticle diffusion models. The maximum experimental adsorption capacity was of 255 mg/g at pH 5, whereas the data fitted the Sips isotherm:

$$[MO]_{ad,e} = \frac{[MO]_{ad,m} K_S [MO]_{aq,e}^{ns}}{1 + K_S [MO]_{aq,e}^{ns}}$$

(11)

where K_S represented to the equilibrium constant , and ns to a surface heterogeneity parameter. Desorption was investigated using 0.1 M HCl solutions, thus, due to the electrostatic repulsion the dye was removed from the adsorbent. After ten cycles, the adsorbent maintained its desorption performance, though the adsorption rate decreased from 100% to 60%, this decrease was attributed to loss of adsorbent due to agitation and material management.

A graphitic carbon nitride was developed to be used to decrease the contamination produced by diverse compounds, including dyes [49]. The investigation was focused in the removal of methylene blue from aqueous solutions. The dye was removed from the solution very quickly, in the order of seconds, without any additional physical or chemical activation. No desorption data included in the work.

Using zirconium, a Zr-based metal-organic framework was synthesized solvothermally. The adsorptive characteristics of such material were investigated against the presence of methyl red and methylene blue in solution [50]. Experiments showed that a change in activation solvent and activation method altered the physical properties of the adsorbent (surface area, pore-volume, pore diameter, and surface charge), and thus, the capacity to remove the dyes was also altered, some of the experimental results were summarized in Table 4.

Table 4. Performance of the adsorbent at various activation and methods of activation

Adsorbent	Activation	Method	Days of activation	% MB adsorption	% MR adsorption
AS-5	acetone	Soxhlet	5	19	93
CS-5	chloroform	Soxhlet	5	62	82
ES-5	ethanol	Soxhlet	5	41	95
AC-5	acetone	centrifugation	5	43	90
CC-5	chloroform	centrifugation	5	80	94
EC-5	ethanol	centrifugation	5	44	85

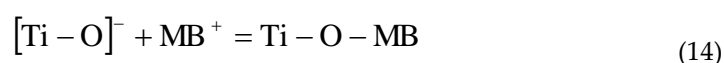
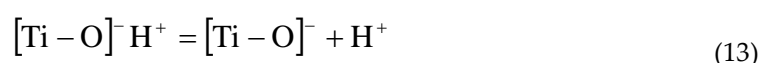
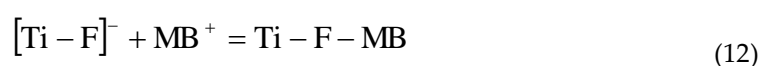
The adsorption of methylene blue increased with the increase of the pH value, with a maximum capacity of 217 mg/g, whereas that of methyl red reached a maximum at pH

2 (243 mg/g), thus, controlling the pH of the solution, the adsorbent can be used to separate selectively one from another. In both cases, adsorption followed the Langmuir and pseudo-second order kinetic models, also the adsorption was spontaneous and endothermic. Desorption used acidic ethanol solutions under ultrasonic assistant during one hour as desorbent procedure. After five cycles, a slight decrease in the adsorption capacity was shown either for methyl red and methylene blue dyes.

One-step hydrothermal method allowed to the production of flower-like Mg/Fe-layered double oxide nanospheres, the adsorbent was used to decrease methyl blue and Congo red levels in aqueous solutions [51]. The remove of 99% initial dye concentration was quick in the case of methyl blue, 5 min, but took about 25 min in the case of Congo red. Following the Langmuir isotherm, in the 20°-40° C range, maximum removal capacities (25° C) varied from 1250 mg/g in the case of Congo red, and 2000 mg/g for methyl blue; these results were attributable to the chemical adsorption, between both anionic dyes and cationic adsorbent nanospheres, through strong electrostatic interactions. The adsorption of both dyes followed the pseudo-second order kinetic model, in endothermic and spontaneous adsorption processes. In the case of methyl blue, desorption was done by water (three washes), and the adsorption efficiency (above 99%) was maintained for five cycles.

Cobalt ferrite nanoparticles capped with an ultrathin phosphate layer of near 1 nm thick were synthesized and characterized using usual techniques [52], and used in the adsorption of a number of dyes. These capped nanoparticles adsorbed 4.5 mg/g (89.5 % adsorption) of methylene blue within 5 min, value which compared well with the practically non-adsorption of the dye using uncoated cobalt ferrite. Using solutions of 50 mg/L of the corresponding dye, the adsorption efficiency for various of these dyes were: brilliant blue R (92%), bromo phenol blue (75%) and methylene blue (91%). No desorption data included here..

The next investigation showed the abilities of F-terminated $\text{Ti}_3\text{C}_2\text{T}_x$ MXene as adsorbent of methylene blue-bearing wastewater [53]. The adsorption efficiency towards this dye sharply decreased from pH 4 to pH 7, with maximum adsorption achieved at pH 2. The adsorption was based in the next reactions:



thus, F and O terminations attracted methylene blue molecules. Other dyes (methyl orange and rhodamine B) can be also adsorbed, though the adsorption was dependent on the exposure time, increasing with the time in the case of the above dyes. The removal efficiency of methylene blue slightly decreased from the first to the fourth cycle.

It was investigated the in-situ growth of zeolitic imidazolate frameworks on zinc layered double hydroxide, which developed in a porous composite material (ZIF-8@ZnAl-LDH) [54]. Thus material was used in the removal of malachite green and methyl orange from water. In both cases, adsorption equilibrium was reached after two hours, and followed the Langmuir isotherm. Due to the nature of these dyes, the pH influenced their adsorption in contrary manner: an increased of the pH from 2 to 10 favoured the adsorption of malachite green, whereas methyl orange was best removed from the solution at acidic pH values (e.g. 3). Ethanol was effective in the desorption of both dyes, and after four consecutive cycles, the adsorbent maintained a 97% and 95% adsorption rate for malachite green and methyl orange, respectively, of its initial adsorption capacity.

These results were attributable to the adsorbent characteristics: i) greater superficial area, ii) porous structure, and iii) exposed metallic nodes within the specific morphological inter-layered structure.

A material formed by polystyrene sulfonate on a laterite soil was investigated to adsorb crystal violet and methylene blue from aqueous solution [55]. Both dyes were effectively removed from the solution after 75 min, at pH values of 8 (crystal violet) or 9 (methylene blue), also in both cases, the adsorption efficiency increased from pH 2 to alkaline values. The adsorption data derived from both dyes, indicated exothermic and spontaneous adsorption processes, and fitted well to the Langmuir model, being the capacity, in a solution of ionic strength 1mM, about 43 mg/g (crystal violet) and 14 mg/g (methylene blue). Desorption data were absent in the investigation.

A biosynthesis strategy using MgO nanoparticles and various Tecoma stans (L.) plant extracts (flower, bark, and leaf), was developed in order to find a suitable adsorbent for organic dyes [56]. The investigated dyes were Congo red and crystal violet, and the variables investigated were: pH, time, and dye concentration. Best conditions for Congo red uptake (99.7%) were: pH 7.9, concentration 9.3 mg/L, whereas crystal violet was adsorbed (90.8%) at a pH value of 6.3, concentration of 5 mg/L. Maximum adsorption capacities were yielded when the adsorbent derived when flower extract was used, and they varied from 89 (Congo red) to 150 mg/g (crystal violet). The adsorption of both dyes followed the Langmuir isotherm and the pseudo-second order kinetic model. Under continuous use of three cycles, there was a continuous decrease in the effectiveness of both adsorption-desorption operations.

Akaganeite nanoparticles (average size 50 nm) were synthesized by using microwave, and use to remove Congo red from an aqueous phase [57]. Experimental results showed that the adsorption kinetics fitted the non-linear pseudo-second-order equation, whereas adsorption equilibrium values, at various temperatures, generally best fitted to non-linear Langmuir isotherm, being the maximum adsorption capacity of more than 150 mg/g at pH 5.5.. The dye uptake onto the adsorbent was spontaneous and endothermic. No desorption data were included in the work.

A natural bentonite was used as adsorbent to remove basic red 46 from aqueous solution [58]. Throughout the experimentation, an adsorbent concentration of 0.1 g/L was used. At pH 7 and 25° C, the maximum adsorption capacity was of 594 mg/g, being the experimental data best fitted to the Langmuir isotherm and pseudo-second order kinetic model. The increase of the temperature was associated to a decrease of dye uptake onto the adsorbent. Investigations about the desorption step were not included in the work.

Again using metal organic frameworks, two mixed compounds: $\{[\text{Zn}_2(5\text{NO}_2\text{-IP})_2(\text{L})_2](\text{H}_2\text{O})\}_n$, named ADES-1, and $\{[\text{Cd}_2(5\text{NO}_2\text{-IP})_2(\text{L})_2(\text{H}_2\text{O})_4](\text{L})(\text{H}_2\text{O})(\text{CH}_3\text{OH})_6\}_n$, named ADES-2, and where 5NO₂-IP = 5-nitroisophthalate and L = (E)-N'-(pyridin-3-ylmethylene)nicotinohydrazide), had been synthesized and characterized via normal techniques [59]. ADES-1 allowed to the rapid and efficient adsorption of both cationic and anionic dye molecules, though it showed a preference for methyl violet (86% adsorption), if compared to the other dyes that were investigated, with some of the results summarized in Table 5.

Table 5. Adsorption of dyes by ADES-1

Dye	Removal efficiency, %	[Dye] _{ad.e} , mg/g
methyl violet	86	1.8
methylene blue	80	1.7
rhodamine B	60	1.3
methyl orange	54	0.99

Initial dye concentration: 5×10^{-5} M. Time: 3 hours

The usefulness of ADES-1 in the separation of a mixture of dyes and its use in a column for the same purpose were also investigated. Desorption was investigated using methanol and 90 min of reaction time.

An adsorbent of conjugated sponge of karaya gum and chitosan had been synthesized and used in the removal of anionic and cationic dyes from aqueous solutions [60]. Result from the investigation showed that the adsorbent presented an adsorption capacity of 33 mg /g for methyl orange, and also 33 mg/g in the case of methylene blue. The aqueous pH value influenced the adsorption of methylene blue, decreasing it as the pH was increased from 5 to 10. Methyl orange uptake responded well to the Langmuir isotherm, indicating adsorption on homogeneous surface, against, methylene blue adsorption fitted to the Freundlich isotherm, being indicative of an adsorption onto a heterogeneous surface; both dyes, in the concentration range of 10-50 mg/L), followed the pseudo-second-order equation. Adsorption was caused by electrostatic interaction between SO_3^- groups of methyl orange and NH_3^+ groups in the adsorbent, in the case of methylene blue, the interactions were between N^+ groups in the dye and COO^- groups present in the adsorbent. Desorption was carried out with 0.1 M HCl (methylene blue) or 0.1 M NaOH (methyl orange). It was shown a slight but continuous decrease (six cycles) in the adsorption-desorption rates.

In the race to find low-cost adsorbents, a non-toxic biosorbent possessing high charge density and thermal stability was prepared by using hexametaphosphate as ionic cross-linker. The as-obtained chitosan microspheres were used in the removal of malachite green and anionic reactive red-195 from waters [61]. And whereas the adsorption equilibrium was fixed at 120 min (malachite green) or 60 min (reactive red-195), the adsorption was best described, in the 25°-45° C), by the pseudo-second-order model, Freundlich and Temkin isotherms. Studying the influence of the temperature on dyes adsorption, it was showed the exothermic and non-spontaneous (malachite green) and endothermic and spontaneous (reactive red-195) nature of the adsorption processes. No desorption data included in the work.

A composite material of magnetic crosslinked chitosan-glyoxal/ $\text{ZnO}/\text{Fe}_3\text{O}_4$ nanoparticles (CS-G/ $\text{ZnO}/\text{Fe}_3\text{O}_4$ NPs) was used in the adsorption of reactive blue 19 [62]. The compound was firstly produced by first Schiff's base magnetic crosslinked chitosan-glyoxal/ Fe_3O_4 composite (CS-G/ Fe_3O_4) synthesis, and further loading of zinc oxide nanoparticles into the polymeric matrix. Using dye concentrations in the 50-300 mg/L range, the adsorption results were well described by the pseudo-second order kinetic model and Freundlich isotherm, being the maximum adsorption capacity of 363 mg/g at 60 °C. Dye uptake was attributable to several types of interactions: i) electrostatic attractions, ii) hydrogen bonding, and iii) $n-\pi$ interactions. Again, the desorption step was not considered in the work.

A type of hierarchical porous zeolitic imidazole frameworks -67@ layered double hydroxide, ZIF-67@LDH, was developed; the material consisted of nanocubes decorated with nanosheets [63]. This material was used in the adsorption of methyl orange and alizarin red S at various pH values, temperatures, and contact time. Adsorption equilibrium was attained within 100 min at 30° C, with a slight increase of the adsorption capacity with the increase of the temperature (20-40° C). The adsorption followed the pseudo-second order kinetic model and the Langmuir isotherm, which confirmed the monolayer adsorption of the dye onto the adsorbent. Maximum capacities were of 793 mg/g and pH 4 (alizarin red S) and 316 mg/g and pH 6 (methyl orange). Desorption was accomplished by the use of 0.1 M HCl solution followed with a second wash with ethanol and water. After four cycles, the adsorbent presented a continuous decrease in its adsorption capacity.

The material, Ag@ZIF-67, was used in the removal of methyl orange from polluted water [64]. Dye uptake increased from pH 2 to pH 6, with a further decrease until pH 11, this uptake also increased with temperature in the 10-30° C range, with no variation at 40°

C. The experimental data fitted to the pseudo-second order kinetic and Langmuir models, with a maximum adsorption capacity of 1146 mg/g. Dye desorption used 0.1 M HCl solutions, a continuous decrease in the adsorption-desorption capacity was observed, e.g. 99% adsorption (first cycle) against 70-80% (fifth cycle).

Synthetic and functionalized amorphous silica, silica nanosheets and silica nanoparticles, modified by hexadecyl trimethyl ammonium bromide, and hexadecyl trimethoxysilane were used to remove dyes from solutions [65]. The investigated dyes were malachite green, crystal violet and bromophenol blue. In the case of malachite green, the dye uptake increased with the pH value from 3 to 9, whereas for crystal violet and bromophenol blue the adsorption was better in the 5-9 pH values range. Typical uptakes were 423 mg/g (malachite green), 409 mg/g (crystal violet) and 262 mg/g (bromophenol blue). Experimental data fitted to the pseudo-second-order and Freundlich models, attributable to the significant role of π - π stacking. No desorption data included in the work.

In the next investigation, a microporous anionic metal organic framework, JUC-210, was synthesized using a spirobifluorene-based ligand and In(III) [66]. Due to its structure, which consisted in a two-fold interpenetrated pts framework with a large void space, the material was investigated to separate various dyes. The adsorbent showed a high selective adsorption towards methylene blue, and in the presence of neutral red, Sudan I, Orange II and methyl orange. The adsorption of methylene blue followed the Lagmuir and the pseudo-second order kinetic models, and its adsorption, due to its positive charge, was based on ion exchange and size exclusion. The desorption step was not considered in the work.

Since pristine carbon materials poorly removed organic dyes from waters, tuning the carbon with magentics compounds tended to reverse the above situation. Thus, carbon biomass from the seeds of *Moringa oleifera* was mixed with manganese ferrite, and the final material was investigated to adsorb indigo carmine, acid blue 158 and reactive blue 4 [67]. Dyes uptake onto the adsorbent was 34 mg/g, 35 mg/g and 32 mg/g for the above dyes, respectively, being the maximum adsorption occurred at pH near 3. Also in the three cases, the adsorption followed the pseudo-second order model and the Freundlich isotherm, in endothermic and spontaneous processes. In the presence of co-existing anions, chloride, sulphate or bicarbonate, the adsorption slightly decreased, being this attributable to competence with the dye molecules for vacant sites of the adsorbent. The adsorbent worked via electrostatic attraction, hydrogen bonding and π - π interaction. Desorption was performed using a 0.1 M NaOH solution, with a relationship of 50 mL desorption solution/100 mg of adsorbent loaded with dye. After five cycles, the efficacy of the adsorbent decreased, probably due to the increasing clustering of the adsorbent surface. Some of these results were shown in Table 6.

Table 6. Efficacy of the adsorbent after cycles of adsorption-desorption

Dye	1st cycle	2nd cycle	3rd cycle	4th cycle	5th cycle
reactive blue 4	85	83	70	65	60
indigo carmine	90	85	80	73	65
acid blue 158	93	85	80	65	63

Alginate reinforced reduced graphene oxide@hydroxyapatite hybrids had been synthesized via co-precipitation method, and investigated as adsorbent towards reactive blue 4, acid blue 158 and indigo carmine from aqueous solution [68]. The corresponding uptake was of 46 mg/g, 48 mg/g and 47 mg/g, respectively. Within this adsorbent, the pH value to generate maximum adsorption was 6-7, and the dyes removal was endothermic and spontaneous. The presence of bicarbonate in the solution did not affect the adsorption properties, however, if chloride or sulphate anions were presented in the

water, the adsorption efficiency decreased, due to interactions with the adsorbent surface. Dyes uptake was attributable to i) electrostatic interactions, ii) surface complexation and iii) hydrogen bonding mechanisms. Desorption was carried out with 0.1 M NaOH solutions, decreasing in a continuous for the adsorption capacity from the first to the fifth cycle.

Methylene blue and methyl orange were adsorbed using a three-dimensional graphene aerogel material, fabricated from graphene oxide sheets with ethylenediamine acting as a reducing agent [69]. Maximum adsorption capacities were of 222 mg/g (methylene blue) and 167 mg/g (methyl orange). The adsorption followed the Langmuir isotherm and the pseudo-second order kinetic model, being the maximum adsorption reached at pH 6 (methylene blue) or pH 3 (methyl orange). Adsorption equilibrium was reached at very different times: 250 min in the case of methyl orange, or near 800 min for methylene blue. No desorption data appeared in the work.

A mixed compound of nitrilotriacetic acid β -cyclodextrin-chitosan was produced for the simultaneous removal of dyes and metals [70]. In this adsorption process, β -cyclodextrin cavities adsorbed methylene blue by host/guest contacts, and the remaining functional groups acted as adsorption sites for methyl orange (and metal ions). Maximum adsorption capacities of the adsorbent were 133 mg/g (methyl orange), 163 mg/g (methylene blue). The adsorption data fitted to Sips (methyl orange) and Langmuir (methylene blue) models, following the adsorption of both dyes the pseudo-second order kinetic model. Desorption was accomplished with HCl, ethanol or nitric acid, followed by washing with deionized water. In binary solutions containing methylene blue and Hg(II), the removal efficiency for the dye was maintained nearly constant (95%) after four cycles.

As it was mentioned above, pristine carbon materials tended to have low dyes removal capacity, one method to improve this fault was to tune the carbonaceous material with a complementary one. One type of material that can be added was biomaterials. In the next reference, a sulfur tethered adsorbent of chitosan-tapioca peel biochar composite was fabricated. The peel of tapioca acted as a precursor for the fabrication of the biochar matrix. The removal of malachite green and rhodamine B from solutions using this adsorbent was investigated [71]. Using dyes concentrations of 50 mg/L, the uptakes were of 53 mg/g (malachite green) and 41 mg/g (rhodamine B), at a pH near 8 and after 120 min. The adsorption followed the pseudo-second-order kinetics and Langmuir isotherm equations. As it was being the norm, dyes adsorption was attributable to i) electrostatic attractions, ii) hydrogen bonding and iii) π - π interactions. Using 0.1 M NaOH solutions to desorb the loaded dyes, the adsorbent was used in five successive cycles of adsorption-desorption with a continuous decrease in its properties to remove the dyes from the solution.

In a very similar investigation than above [71], the same adsorbent and dyes were used, though in this case [72], the dyes concentrations were 25 mg/L, and this is because dyes uptake were lower than in the previous reference, 30 mg/L versus 53 mg/g (malachite green) or 33 mg/g versus 41 mg/g (rhodamine B), also best uptakes were yielded at pH near 8 and after 120 min of reaction. The experimental data also followed the pseudo-second-order kinetic model, but in this case, the adsorption fitted to the Freundlich isotherm instead of the Langmuir one. The adsorbent also lost its properties under five cycles of adsorption-desorption.

$\text{Zn}_3(\text{OH})_2\text{V}_2\text{O}_7 \cdot 2\text{H}_2\text{O}$ nanocables had been fabricated by a DL-Alanine assisted hydrothermal route, and used in the adsorption of methylene blue [73]. The maximum adsorption capacity was of 113 mg/g at 25° C, in a physisorption process, following the pseudo-second order equation and the Langmuir isotherm. No desorption data included in the work.

Zeolitic imidazolate framework-67 was used as template to fabricate hollow LDH nanocages, the template was consumed during the formation of the nanomaterial. The nanocages were composed of NiCo-LDH nanosheets which maintained the dodecahedron shape of the template [74]. The resultant material was used to remove

Congo red under various experimental variables. Dye adsorption was attributable to a chemisorption process, and followed the pseudo-second order kinetic model and the Langmuir isotherm in the 25-45° C temperatures range. With maximum adsorption at pH 7, the maximum capacity increased with the increase of the temperature, e.g. 926 mg/g (25° C) or 1197 mg/g (60° C). The nanocages can be regenerated through solvothermal method using methanol, and treated qt 80° C during 12 hours. Continuous use of the adsorbent demonstrated that there was a slight but continuous loss of the adsorptive capacity up to five cycles.

A mixed process of biomodification and magnetic treatment was used to prepare polydopamine-modified graphene-based adsorbent, which incorporated active Fe3O4 nanoparticles (average size of 6.5 nm) [75]. With an increase of the adsorption capacity from pH 2 to 10, the adsorption equilibrium was reached after seven hours. The adsorption of methylene blue followed the pseudo-second-order kinetic model, and the intraparticle diffusion model, as well as the Langmuir isotherm. Maximum adsorption capacities were of 132 mg/g (30° C), 140 mg/g (40° C), and 152 mg/g (50° C), being the adsorption endothermic and spontaneous, also it showed an increase in the randomness at the solid-solution interface. Desorption followed an acid treatment to induce dye removal from the adsorbent, being this caused by the generation of an excess of protons which competed with the cationic dye and endow the amine groups of the adsorbent with a positive charge with the subsequent repulsion the dye molecule. After five cycles, the adsorbent showed a continuous decrease of its initial removal rate.

Melamine and cyanuric chloride were directly used to fabricate by a polycondensation a covalent triazine framework; due to its properties: numerous basic nitrogen atoms (near 59% wt %), BET surface area (670 m/g), and hierarchical pore structure, the material was investigated as potential adsorbent of anionic dyes, taking as example the removal of Congo red [76]. The maximum adsorption capacity was of 1581 mg/g at 30 °C, being the adsorption mechanism attributable to the electrostatic attraction and hydrogen bonding between the dye and the adsorbent. As can be seen from Table 7, the adsorbent lost its effectiveness as the pH value was increased.

Table 7. Influence of the pH on the adsorption of anionic and cationic dyes

Dye	Type	pH	[dye] _{ad,m} , mg/g
Congo red	anionic	5	1581
		12	600
Rhodamine B	cationic	5	370
		12	250

Temperature: 30° C. Time: 12 h. Dye concentrations: 60 mg/L. Adsorbent dosage: 30 mg/L

The adsorption of cationic dyes can be improved when used mixed with Congo red, e.g. single cationic dye solutions of malachite green or methylene blue resulted in an adsorption rate of 57% or 16%, respectively; however, the binary mixture of these with Congo red resulted in an 100% (malachite green) or 92% (methylene blue) adsorption rates. This synergistic effect was attributed to i) the preferential adsorption of Congo red onto the adsorbent surface reduced the surface charge, tus, this surface was more adequate to adsorb cationic molecules, and ii) sulfonic groups in the Congo red molecule reacted with the positive groups (e.g. quaternary ammonium group) presented in the cationic compound enhancing their removal from the solution, that is, Congo red acted as a bridge between the adsorbent ant the cationic molecule. Congo red can be desorbed with the use of a sodium chloride saturated ethanol solution for four hours, the adsorption efficacy decreased from 100% to 90% after six cycles. Moreover monolithic aerogels were produced by incorporating the adsorbent into polyvinylidene fluoride, and a further casting in melamine resin foams.

Another adsorbent-based metal organic framework, this time, nanometer blocks of amide-functionalized Fe(III)-based metal-organic framework were produced, via ultrasonic method and without the addition of any surfactants, at room temperature and atmospheric pressure [77]. It was used in the removal of methylene blue for solution. No desorption data included in the work.

The cyclomatrix phosphazenes-co-3,3'-sulfonyldianiline PSD-NH₂ microspheres was used to remove methyl orange from solutions [78]. As it was being usual in this type of investigation, several variables were considered in the study: pH, adsorbent dosage, contact time, initial dye concentration and temperature. The experimental data indicated that the adsorption capacity of the microspheres was 187 mg/g under the optimal adsorption conditions, and followed the pseudo-second-order kinetic and Langmuir isotherm models. Congo red was adsorbed due to i) intermolecular electrostatic interaction, ii) hydrogen bond between the microspheres adsorbed on the surface and the dye, and iii) π - π and C-H... π stacking and other molecular forces. Dye uptake was endothermic and spontaneous in nature. Desorption data were not included in the work. Attapulgit modified with 3-aminopropyltriethoxysilane were used in the adsorption of Congo red from waters [79]. It was described that pseudo-second-order equation and Sips model best fitted the experimental data. Contrary to the attapulgit behavior, the adsorption via the modified attapulgit was not affected neither by the increase of the temperature nor by the change in the pH value. Desorption was not considered here.

A β -cyclodextrin/graphene oxide composite was prepared by modifying graphene oxide via β -cyclodextrin crosslinking method [80]. The composite was used to investigate its possibilities in the removal of methylene blue from aqueous solution. Under the optimal conditions of temperature (70° C), time (60 min) and adsorbent dosage (0.04 g/L); at pH 7, a removal efficiency of 90% was achieved, which compared well than that of the graphene oxide (70%). The maximum adsorption capacity was 76 mg/g, and the dye was remove from the adsorbent by desorption with absolute alcohol during 12 hours. Removal efficiency was maintained about 90% after nine cycles.

The next reference investigated the removal of methylene blue and orange green by a series of adsorbents polymers [81]. The adsorption of methylene blue reached the equilibrium after 45 min at pH 6.86 and 20° C. This reference is unique because it included an approach to the cost of the adsorbents studied on the removal of dyes, Table 8 presented some of these results.

Table 8. Approximate costs in the removal of methylene blue from solution using various adsorbents

Adsorbent	Adsorbent cost, US dollars	Methylene blue capacity, mol/g
wheat flour	<5	3.3
turmeric powder	10	6.8
polyaniline	25-30	7.1
nano(Fe-Ni-Si) oxide	near 10	22

Treatment of 1000 L of a synthetic solution containing 1x10⁻⁵ M dye. No desorption data were included in the reference.

Jute fiber was subjected to a chemical activation method to yield activated carbon fibers [9]. The as-prepared material was used to investigate its adsorbent properties against methylene blue and 4-nitrophenol.

A foam, described as GO/g-C₃N₄/TiO₂ was prepared via hydrothermal treatment and freeze-drying methods [82]. Besides oil-water mixtures, this material was used to adsorb organic dyes such as: rhodamine B, methylene blue and methyl orange; both rhodamine B and methylene blue were adsorbed with efficiencies near 98%, whereas in a mixture of methylene blue and methyl orange, the cationic dye was totally adsorbed by the foam

but methyl orange was maintained in the solution. No desorption data were included in the investigation.

Being *Physalis alkekengi* L. husk an agricultural waste product, its disposal caused environmental pollution of water and air. Thus, in order to give a further utility to this waste, it was used as precursor of a porous carbon material. Malachite green was used to investigate the adsorption properties of the material [83]. It was found that a pH of 9, the maximum adsorption capacity of the adsorbent reached near 2000 mg/g, whereas 51% (1016 mg/g) of the dye was adsorbed in the first five minutes. Dye uptake followed the pseudo-second order and the Bangham models:

$$[MG]_{ad,t} = [MG]_{ad,e} \left(1 - e^{-K_4 t^n}\right) \quad (15)$$

where K_4 represented to the Bangham rate constant, and n to the power of the Bangham model. The increase of the temperature, in the 20-40° C range, produced a slight increase in the adsorption capacity, which followed the Langmuir model. Deionized water was used to desorb the dye, and the adsorbent was recarbonized at 600° C under nitrogen atmosphere. After ten cycles the adsorbent decrease its removal rate from 100% to 89%, though further recycling caused a slight decrease in the adsorption capacity, probably caused by the deposition of byproducts on the adsorbent surface.

Hydrothermal procedures were used to fabricate coordination polymeric chains modified polyoxometalate, $H_3K_2[Ag_5(DTB)_5][SiW_{12}O_{40}]_2 \cdot Cl_2 \cdot 8H_2O$, where {DTB = 1,4-di(1H-1,2,4-triazol-1-yl)benzene} [84]. In single solutions, the removal rate for crystal violet was 74% after 90 minutes, in the same time, 85% of methylene blue was removed from the solution. Using binary solutions, the material can separate in selective form methylene blue and crystal violet from methyl orange; that is, cationic dyes from anionic ones. The data indicated that this adsorption was attributable to the sizes of organic dyes. No desorption data included in the manuscript.

A titanate-based materials (peroxide sodium titanate, PST) was used as precursor to fabricate three types of surface charged surfactant: dodecyl dimethyl betaine (BS-PST), sodium dodecyl sulphate (SDS-PST) and dodecyltrimethyl ammonium chloride (DTAC-PST) [85]. These were used to investigate the removal of contaminants such as methylene blue, acid red G as well as ammonia nitrogen and phosphate. Batch experimentation showed that DTAC-PST material had the best removal performance over methylene blue, though the maximum adsorption capacity was of 82 mg/g (methylene blue) and 546 mg/g (acid red G). In simulated waters containing 50 mg/L methylene blue and 50 mg/L acid red G, plus the inorganic contaminants mentioned above, the dyes concentrations in the solution, at the equilibrium, were maintained below the limiting value of 10 mg/L, marked by the discharge levels in China (GB, 18918–2002), by using the adsorbent and controlling the pH value: 2-4 for acid red G, or 2-10 for methylene blue. Electrostatic attraction and ligand exchange were the mechanism of methylene blue uptake onto the adsorbent reason, whereas in the case of acid red G, C-N⁺ from DTAC modification was the responsible for the adsorption of the dye. The dye-loaded DTAC-PST can be regenerated by 0.5 M NaOH solutions, maintaining near 80% of its adsorption capacity after five cycles.

Methylenen blue and rhodamine B were removed from solutions by the use of porous BN nano/microrods [86]. The material also acted in a selective form, towards cationic dyes, in the case of binary mixtures of Congo red and the above cationic dyes. This selectivity was attributable to the synergistic effect of i) electrostatic and π - π interactions, ii) size of the dye molecule and iii) specific surface area and pore size of the adsorbent. The removal of the adsorbed dye from the adsorbent was not included in the investigation.

3. Conclusions

This review demonstrated that, the subject of the removal or hazardous organic dyes from solutions is of a considerable interest for numerous investigation groups and Institutions around the world, however, and as it can be seen in Table 9, this review demonstrated that the experimental investigations, published during the first six months of 2021 year, were mainly polarized in a limiting geographical zone. Effectively, the vast amount of these investigations came from Asia, and within this continent, authors and institutions, also by a great difference over others, came from China.

In this period time, the removal of about 36 different organic dyes had been investigated, however, and as can be seen from Table 10, the quantitative results showed by the papers presented a great disparity in the maximum dye adsorbed capacity resulted from the experimental data.

Table 9. Distribution of the papers published in the first six months of 2021 year

Zone	Percentage ^a
Africa	2.6
America	6.5
Asia	85.7
Europe	3.9
Oceania	1.3

^a Over a total of 77 manuscripts. Distribution based on the address of the corresponding author.

Table 10. Some quantitative results about organic dyes uptake onto different adsorbents

Methylene blue	Malachite green	Methyl orange	Congo red
12	140	6	89
25	2000	133	140
573		255	331
1584		316	926
1690		1146	1250
1807		1409	1581

(Concentrations in mg/g)

From the papers published, an important 39% of them, did not present desorption results, being this less than acceptable, because authors must realized that as important as the adsorption of a given dye onto an adsorbent, the release (desorption step) of the solute from the loaded adsorbent is equally important to know the real practical usefulness of the given adsorbent, that is, only with the adsorption step, one have just a 50% of the information to judge the effectiveness of the adsorbent to remove a dye from solutions.

Also in all the cases, these reviewers detected that no one of the reported investigations mentioned what to do with the desorbed solution containing the desorbed dye, which presumably may have a greater dye concentration that the dye-bearing feed solutions, since normally the desorbed phase used lower volumes than the feed one, and thus, they becomes more concentrated in the dye and consequently they are more hazardous or toxic than initial ones.

Only one [20] of the reviewed manuscripts, investigated about the influence of the stirring speed on the dye uptake onto the adsorbent. This is an experimental variable often

neglected by authors, and may be of the same importance than others, e.g. pH, temperature, dosages, etc., because, as also mentioned in [20], with the correct stirring speed applied on the system, the thickness of the solution boundary layer reached a minimum and the adsorption maximizes. Authors must noted that the influence (or not) of this variable on dye adsorption is not predictable and only can be know after experimentation. Considering the above, must one consider correct the quantitative results given in the manuscripts?.

In any case, the topic about the removal of organic dyes from solutions, by means of adsorption methodologies, still is of a fascinating interest by many research groups, and by no doubt the number of adsorbents to be used in this field is expected to be expanding, and the results, hopefully without the above points, will continue to be published and fulfil our knowledge in this important environmental and sociological issue.

Author Contributions: Conceptualization, F.J.A. and F.A.L.; writing-original draw preparation, F.J.A.; writing-review and editing, F.J.A. and F.A.L.; supervision, F.J.A. and F.A.L. All authors have read and agreed to the published version of the manuscript.

Funding: Please add: This research received no external funding.

Institutional Review Board Statement: Not applicable.

Informed Consent Statement: Not applicable.

Acknowledgments: We acknowledge support of the publication fee by the CSIC Open Access Publication Support Initiative through its Unit of Information Resources for Research (URICI).

Conflicts of Interest: The authors declare no conflict of interest.

References

- [1] Costa, J.A.S.; De Jesus, R.A.; Santos, D.O.; Neris, J.B.; Figueiredo, R.T.; Paranhos, C.M. Synthesis, functionalization, and environmental application of silica-based mesoporous materials of the M41S and SBA-n families: A review. *Journal of Environmental Chemical Engineering* **2021**, *9*, 105259. DOI: 10.1016/j.jece.2021.105259
- [2] Donga, C.; Mishra, S.B.; Abd-El-Aziz, A.S.; Mishra, A.K. Advances in graphene-based magnetic and graphene-based/TiO₂ nanoparticles in the removal of heavy metals and organic pollutants from industrial wastewater. *Journal of Inorganic and Organometallic Polymers and Materials* **2021**, *31*, 463–480. DOI: 10.1007/s10904-020-01679-3
- [3] Yap, P.L.; Nine, M.J.; Hassan, K.; Tung, T.T.; Tran, D.N.H.; Losic, D. Graphene-based sorbents for multipollutants removal in water: a review of recent progress. *Advanced Functional Materials* **2021**, *31*, 2007356. DOI: 10.1002/adfm.202007356
- [4] Gautam, R.K.; Goswami, M.; Mishra, R.K.; Chaturvedi, P.; Awasthi, M.K.; Singh, R.S.; Giri, B.S.; Pandey, A. Biochar for remediation of agrochemicals and synthetic organic dyes from environmental samples: A review. *Chemosphere* **2021**, *272*, 129917. DOI: 10.1016/j.chemosphere.2021.129917
- [5] Parmar, B.; Bisht, K.K.; Rajput, G.; Suresh, E. Recent advances in metal-organic frameworks as adsorbent materials for hazardous dye molecules. *Dalton Transactions* **2021**, *50*, 3083–3108. DOI: 10.1039/d0dt03824e
- [6] Yuan, N.; Gong, X.; Sun, W.; Yu, C. Advanced applications of Zr-based MOFs in the removal of water pollutants. *Chemosphere* **2021**, *267*, 128863. DOI: 10.1016/j.chemosphere.2020.128863
- [7] Thamer, B.M.; Aldalbahi, A.; Meera Moydeen, A.; Rahaman, M.; El-Newehy, M.H. Modified electrospun polymeric nanofibers and their nanocomposites as nanoadsorbents for toxic dye removal from contaminated waters: A review. *Polymers* **2021**, *23*, 20. DOI: 10.3390/polym13010020
- [8] Xiao, W.; Jiang, X.; Liu, X.; Zhou, W.; Garba, Z.N.; Lawan, I.; Wang, L.; Yuan, Z. Adsorption of organic dyes from wastewater by metal-doped porous carbon materials. *Journal of Cleaner Production* **2021**, *284*, 124773. DOI: 10.1016/j.jclepro.2020.124773

- [9] Yousuf, M.R.; Mahnaz, F.; Syeda, S.R. Activated carbon fiber from natural precursors: A review of preparation methods with experimental study on jute fiber. *Desalination and Water Treatment* **2021**, *213*, 441-458. DOI: 10.5004/dwt.2021.26731
- [10] Adel, M.; Ahmed, M.A.; Mohamed, A.A. Synthesis and characterization of magnetically separable and recyclable crumbled MgFe₂O₄/reduced graphene oxide nanoparticles for removal of methylene blue dye from aqueous solutions. *Journal of Physics and Chemistry of Solids* **2021**, *149*, 109760. DOI: 10.1016/j.jpcs.2020.109760
- [11] Ahmadipouya, S.; Heidarian Haris, M.; Ahmadijokani, F.; Jarahiyan, A.; Molavi, H.; Matloubi Moghaddam, F.; Rezakazemi, M.; Arjmand, M. Magnetic Fe₃O₄@UiO-66 nanocomposite for rapid adsorption of organic dyes from aqueous solution. *Journal of Molecular Liquids* **2021**, *322*, 114910. DOI: 10.1016/j.molliq.2020.114910
- [12] Chen, M.; Shen, Y.; Xu, L.; Xiang, G.; Ni, Z. Highly efficient and rapid adsorption of methylene blue dye onto vinyl hybrid silica nano-cross-linked nanocomposite hydrogel. *Colloids and Surfaces A: Physicochemical and Engineering Aspects* **2021**, *613*, 126050. DOI: 10.1016/j.colsurfa.2020.126050
- [13] Chen, X.; Li, S.-B.; Liu, Z.-Y.; Zhang, Y.-T. Solvent-directed assembly of Zr-based metal-organic cages for dye adsorption from aqueous solution. *Journal of Solid State Chemistry* **2021**, *296*, 121998. DOI: 10.1016/j.jssc.2021.121998
- [14] Cui, Z.; Lin, H.; Zeng, L.; Lu, J. A new functionalized POM-based MOF containing 1D [Mo₃O₁₀]ⁿ⁻²ⁿ chains and the flexible bis(pyrazine)-bis(amide) ligand. *Inorganic Chemistry Communications* **2021**, *126*, 108493. DOI: 10.1016/j.inoche.2021.108493
- [15] Da'na, E.; Taha, A.; Hessien, M. Application of ZnO–NiO greenly synthesized nanocomposite adsorbent on the elimination of organic dye from aqueous solutions: Kinetics and equilibrium. *Ceramics International* **2021**, *47*, 4531-4542. DOI: 10.1016/j.ceramint.2020.10.015
- [16] Delpiano, G.R.; Tocco, D.; Medda, L.; Magner, E.; Salis, A. Adsorption of malachite green and alizarin red s dyes using fe-btc metal organic framework as adsorbent. *International Journal of Molecular Sciences* **2021**, *22*, 788. DOI: 10.3390/ijms22020788
- [17] Deng, F.; Liang, J.; Yang, G.; Huang, Q.; Dou, J.; Chen, J.; Wen, Y.; Liu, M.; Zhang, X.; Wei, Y. Direct generation of poly(ionic liquids) on mesoporous carbon via Diels-Alder and multicomponent reactions for ultrafast adsorptive removal anionic organic dye with high efficiency. *Journal of Environmental Chemical Engineering* **2021**, *9*, 104872. DOI: 10.1016/j.jece.2020.104872
- [18] Ding, R.-D.; Li, D.-D.; Yu, J.-H.; Jia, M.-J.; Xu, J.-Q. Porous 3,4-di(3,5-dicarboxyphenyl)phthalate-based Cd²⁺ coordination polymer and its potential applications. *Spectrochimica Acta-Part A: Molecular and Biomolecular Spectroscopy* **2021**, *252*, 119498. DOI: 10.1016/j.saa.2021.119498
- [19] Dong, B.; Wang, W.-J.; Xi, S.-C.; Wang, D.-Y.; Wang, R. A carboxyl-functionalized covalent organic framework synthesized in a deep eutectic solvent for dye adsorption. *Chemistry - A European Journal* **2021**, *27*, 2692-2698. DOI: 10.1002/chem.202003381
- [20] Ebrahimi, A.K.; Sheikhshoaie, I.; Salimi, S.; Arkaban, H. nIn-situ facile synthesis of superparamagnetic porous core-shell structure for dye adsorption. *Journal of Molecular Structure* **2021**, *1228*, 129797. DOI: 10.1016/j.molstruc.2020.129797
- [21] Ehgartner, C.R.; Werner, V.; Selz, S.; Hüsing, N.; Feinle, A. Carboxylic acid-modified polysilsesquioxane aerogels for the selective and reversible complexation of heavy metals and organic molecules. *Microporous and Mesoporous Materials* **2021**, *312*, 110759. DOI: 10.1016/j.micromeso.2020.110759
- [22] El Gaayda, J.; Akbour, R.A.; Titchou, F.E.; Afanga, H.; Zazou, H.; Swanson, C.; Hamdani, M. Uptake of an anionic dye from aqueous solution by aluminum oxide particles: equilibrium, kinetic, and thermodynamic studies. *Groundwater for Sustainable Development* **2021**, *12*, 100540. DOI: 10.1016/j.gsd.2020.100540
- [23] Fatima, B.; Siddiqui, S.I.; Nirala, R.K.; Vikrant, K.; Kim, K.-H.; Ahmad, R.; Chaudhry, S.A. Facile green synthesis of ZnO–CdWO₄ nanoparticles and their potential as adsorbents to remove organic dye. *Environmental Pollution* **2021**, *271*, 116401. DOI: 10.1016/j.envpol.2020.116401

- [24] Feng, M.; Yu, S.; Wu, P.; Wang, Z.; Liu, S.; Fu, J. Rapid, high-efficient and selective removal of cationic dyes from wastewater using hollow polydopamine microcapsules: Isotherm, kinetics, thermodynamics and mechanism. *Applied Surface Science* **2021**, 542, 148633. DOI: 10.1016/j.apsusc.2020.148633
- [25] Fu, Q.; Lou, J.; Zhang, R.; Peng, L.; Zhou, S.; Yan, W.; Mo, C.; Luo, J. Highly effective and fast removal of Congo red from wastewater with metal-organic framework Fe-MIL-88NH₂. *Journal of Solid State Chemistry* **2021**, 294, 121836. DOI: 10.1016/j.jssc.2020.121836
- [26] Galan, J.; Trilleras, J.; Zapata, P.A.; Arana, V.A.; Grande-Tovar, C.D. Optimization of chitosan glutaraldehyde-crosslinked beads for reactive blue 4 anionic dye removal using a surface response methodology. *Life* **2021**, 11, 85. DOI: 10.3390/life11020085
- [27] Guo, G.; Zhao, L.; Meng, L.; Liu, X. Structure and performances of three metal coordination polymers synthesized from 4,4'-(phenylazanediy1) dibenzoic acid. *Journal of Molecular Structure* **2021**, 1227, 129053. DOI: 10.1016/j.molstruc.2020.129053
- [28] Guo, Y.; Mo, Y.; Wang, M.; Cui, H.; Tang, Y.; Sun, T. Green and facile synthesis of hierarchical ZnOHF microspheres for rapid and selective adsorption of cationic dyes. *Journal of Molecular Liquids* **2021**, 329, 115529. DOI: 10.1016/j.molliq.2021.115529
- [29] Han, X.; Wang, Y.; Zhang, N.; Meng, J.; Li, Y.; Liang, J. Facile synthesis of mesoporous silica derived from iron ore tailings for efficient adsorption of methylene blue. *Colloids and Surfaces A: Physicochemical and Engineering Aspects* **2021**, 617, 126391. DOI: 10.1016/j.colsurfa.2021.126391
- [30] Hizal, J.; Kanmaz, N.; Yilmazoglu, M. Adsorption efficiency of sulfonated poly (ether ether ketone) (sPEEK) as a novel low-cost polymeric adsorbent for cationic organic dyes removal from aqueous solution. *Journal of Molecular Liquids* **2021**, 322, 114761. DOI: 10.1016/j.molliq.2020.114761
- [31] Jamali, M.; Akbari, A. Facile fabrication of magnetic chitosan hydrogel beads and modified by interfacial polymerization method and study of adsorption of cationic/anionic dyes from aqueous solution. *Journal of Environmental Chemical Engineering* **2021**, 9, 105175. DOI: 10.1016/j.jece.2021.105175
- [32] Kubra, K.T.; Salman, M.S.; Znad, H.; Hasan, M.N. Efficient encapsulation of toxic dye from wastewater using biodegradable polymeric adsorbent. *Journal of Molecular Liquids* **2021**, 329, 115541. DOI: 10.1016/j.molliq.2021.115541
- [33] Kubra, K.T.; Salman, M.S.; Hasan, M.N. Enhanced toxic dye removal from wastewater using biodegradable polymeric natural adsorbent. *Journal of Molecular Liquids* **2021**, 328, 115468. DOI: 10.1016/j.molliq.2021.115468
- [34] Kuk, Y.; Ok, K.M. Novel enantiomeric Pb-coordination polymers dictated by the corresponding chiral ligands, [Pb((R,R)-TBA)(H₂O)]·1.7H₂O and [Pb((S,S)-TBA)(H₂O)]·1.7H₂O [TBA= 1,3,5-triazin-2(1H)-one-4,6-bis(alanyl)]. *Materials Chemistry Frontiers* **2021**, 5, 1330-1340. DOI: 10.1039/d0qm00629g
- [35] Lei, Y.; Huang, Q.; Dou, J.; Huang, H.; Yang, G.; Deng, F.; Liu, M.; Li, X.; Zhang, X.; Wei, Y. Fast adsorptive removal of cationic organic dye by anionic group functionalized carbon nanotubes with high efficiency. *Colloids and Interface Science Communications* **2021**, 40, 100328. DOI: 10.1016/j.colcom.2020.100328
- [36] Li, D.; Chai, K.; Yao, X.; Zhou, L.; Wu, K.; Huang, Z.; Yan, J.; Qin, X.; Wei, W.; Ji, H. β -Cyclodextrin functionalized SBA-15 via amide linkage as a super adsorbent for rapid removal of methyl blue. *Journal of Colloid and Interface Science* **2021**, 583, 100-112. DOI: 10.1016/j.jcis.2020.09.006
- [37] Li, H.; Huang, H.; Yan, X.; Liu, C.; Li, L. A Calix[4]arene-crosslinked polymer for rapid adsorption of cationic dyes in water. *Materials Chemistry and Physics* **2021**, 263, 124295. DOI: 10.1016/j.matchemphys.2021.124295
- [38] Li, J.; Huang, L.; Jiang, X.; Zhang, L.; Sun, X. Preparation and characterization of ternary Cu/Cu₂O/C composite: An extraordinary adsorbent for removing anionic organic dyes from water. *Chemical Engineering Journal* **2021**, 404, 127091. DOI: 10.1016/j.cej.2020.127091

- [39] Li, J.; Shi, C.; Bao, A. Design of boron-doped mesoporous carbon materials for multifunctional applications: dye adsorption and CO₂ capture. *Journal of Environmental Chemical Engineering* **2021**, *9*, 105250. DOI: 10.1016/j.jece.2021.105250
- [40] Li, J.; Wang, B.; Chang, B.; Liu, J.; Zhu, X.; Ma, P.; Sun, L.; Li, M. One new hexatungstate-based binuclear nickel(II) complex with high selectivity adsorption for organic dyes. *Journal of Molecular Structure* **2021**, *1231*, 129674. DOI: 10.1016/j.molstruc.2020.129674
- [41] Lim, S.; Kim, J.H.; Park, H.; Kwak, C.; Yang, J.; Kim, J.; Ryu, S.Y.; Lee, J. Role of electrostatic interactions in the adsorption of dye molecules by Ti₃C₂-MXenes. *RSC Advances* **2021**, *11*, 6201-6211. DOI: 10.1039/d0ra10876f
- [42] Liou, T.-H.; Liou, Y.H. Utilization of rice husk ash in the preparation of graphene-oxide-based mesoporous nanocomposites with excellent adsorption performance. *Materials* **2021**, *14*, 1214. DOI: 10.3390/ma14051214
- [43] Liu, M.; Wang, Z. Adsorption performance of reactive red 2BF onto magnetic Zn_{0.3}Cu_{0.7}Fe₂O₄ nanoparticles. *Materials Research Express* **2021**, *8*, 025014. DOI: 10.1088/2053-1591/abe5f3
- [44] Liu, Q.; Yu, H.; Zeng, F.; Li, X.; Sun, J.; Li, C.; Lin, H.; Su, Z. HKUST-1 modified ultrastability cellulose/chitosan composite aerogel for highly efficient removal of methylene blue. *Carbohydrate Polymers* **2021**, *255*, 117402. DOI: 10.1016/j.carbpol.2020.117402
- [45] Mallakpour, S.; Behranvand, V. Methylene blue contaminated water sanitization with alginate/compact discs waste-derived activated carbon composite beads: Adsorption studies. *International Journal of Biological Macromolecules* **2021**, *180*, 28-35. DOI: 10.1016/j.ijbiomac.2021.03.044
- [46] Manabe, S.; Adavan Kiliyankil, V.; Takiguchi, S.; Kumashiro, T.; Fugetsu, B.; Sakata, I. Graphene nanosheets homogeneously incorporated in polyurethane sponge for the elimination of water-soluble organic dyes. *Journal of Colloid and Interface Science* **2021**, *584*, 816-826. DOI: 10.1016/j.jcis.2020.10.012
- [47] Masud, A.; Zhou, C.; Aich, N. Emerging investigator series: 3D printed graphene-biopolymer aerogels for water contaminant removal: a proof of concept. *Environmental Science: Nano* **2021**, *8*, 399-414. DOI: 10.1039/d0en00953a
- [48] Mendieta-Rodríguez, L.S.; González-Rodríguez, L.M.; Alcaraz-Espinoza, J.J.; Chávez-Guajardo, A.E.; Medina-Llamas, J.C. Synthesis and characterization of a polyurethane-polyaniline macroporous foam material for methyl orange removal in aqueous media. *Materials Today Communications* **2021**, *26*, 102155. DOI: 10.1016/j.mtcomm.2021.102155
- [49] Mohanraj, J.; Durgalakshmi, D.; Saravanan, R. Water-soluble graphitic carbon nitride for clean environmental applications. *Environmental Pollution* **2021**, *269*, 116172. DOI: 10.1016/j.envpol.2020.116172
- [50] Mousavi, D.V.; Ahmadipouya, S.; Shokrgozar, A.; Molavi, H.; Rezakazemi, M.; Ahmadijokani, F.; Arjmand, M. Adsorption performance of UiO-66 towards organic dyes: Effect of activation conditions. *Journal of Molecular Liquids* **2021**, *321*, 114487. DOI: 10.1016/j.molliq.2020.114487
- [51] Mubarak, M.; Islam, M.S.; Yoon, D.-Y.; Lee, J.H.; Park, H.J.; Bae, J.-S.; Lee, H.-J. Flower-like Mg/Fe-layered double oxide nanospheres with ultrahigh adsorption efficiency for anionic organic dyes. *Colloids and Surfaces A: Physicochemical and Engineering Aspects* **2021**, *618*, 126446. DOI: 10.1016/j.colsurfa.2021.126446
- [52] Muthukumaran, T.; Philip, J. Synthesis of water dispersible phosphate capped CoFe₂O₄ nanoparticles and its applications in efficient organic dye removal. *Colloids and Surfaces A: Physicochemical and Engineering Aspects* **2021**, *610*, 125755. DOI: 10.1016/j.colsurfa.2020.125755
- [53] My Tran, N.; Thanh Hoai Ta, Q.; Sreedhar, A.; Noh, J.-S. Ti₃C₂T_x MXene playing as a strong methylene blue adsorbent in wastewater. *Applied Surface Science* **2021**, *537*, 148006. DOI: 10.1016/j.apsusc.2020.148006
- [54] Nazir, M.A.; Bashir, M.A.; Najam, T.; Javed, M.S.; Suleman, S.; Hussain, S.; Kumar, O.P.; Shah, S.S.A.; Rehman, A.U. Combining structurally ordered intermetallic nodes: Kinetic and isothermal studies for removal of malachite green and methyl orange with mechanistic aspects. *Microchemical Journal* **2021**, *164*, 105973. DOI: 10.1016/j.microc.2021.105973

- [55] Ngo, T.M.V.; Nguyen, T.H.L.; Mai, X.T.; Pham, T.H.N.; Nguyen, T.T.T.; Pham, T.D. Adsorptive removal of cationic dyes using hybrid material-based polyelectrolyte modified laterite soil. *Journal of Environmental Chemical Engineering* **2021**, *9*, 105135. DOI: 10.1016/j.jece.2021.105135
- [56] Nguyen, D.T.C.; Dang, H.H.; Vo, D.-V.N.; Bach, L.G.; Nguyen, T.D.; Tran, T.V. Biogenic synthesis of MgO nanoparticles from different extracts (flower, bark, leaf) of *Tecoma stans* (L.) and their utilization in selected organic dyes treatment. *Journal of Hazardous Materials* **2021**, *404*, 124146. DOI: 10.1016/j.jhazmat.2020.124146
- [57] Nguyen, V.D.; Nguyen, H.T.H.; Vranova, V.; Nguyen, L.T.N.; Bui, Q.M.; Khieu, T.T. Artificial neural network modeling for Congo red adsorption on microwave-synthesized akaganeite nanoparticles: optimization, kinetics, mechanism, and thermodynamics. *Environmental Science and Pollution Research* **2021**, *28*, 9133-9145. DOI: 10.1007/s11356-020-10633-2
- [58] Paredes-Quevedo, L.C.; González-Cacedo, C.; Torres-Luna, J.A.; Carriazo, J.G. Removal of a textile azo-dye (Basic Red 46) in water by efficient adsorption on a natural clay. *Water, Air, and Soil Pollution* **2021**, *232*, 4. DOI: 10.1007/s11270-020-04968-2
- [59] Patel, U.; Parmar, B.; Patel, P.; Dadhania, A.; Suresh, E. The synthesis and characterization of Zn(II)/Cd(II) based MOFs by a mixed ligand strategy: A Zn(II) MOF as a dual functional material for reversible dye adsorption and as a heterogeneous catalyst for the Biginelli reaction. *Materials Chemistry Frontiers* **2021**, *5*, 304-314. DOI: 10.1039/d0qm00611d
- [60] Ramakrishnan, R.K.; Padil, V.V.T.; Wacławek, S.; Černík, M.; Varma, R.S. Eco-friendly and economic, adsorptive removal of cationic and anionic dyes by bio-based karaya gum—chitosan sponge. *Polymers* **2021**, *13*, 251. DOI: 10.3390/polym13020251
- [61] Raval, N.P.; Mukherjee, S.; Shah, N.K.; Gikas, P.; Kumar, M. Hexametaphosphate cross-linked chitosan beads for the eco-efficient removal of organic dyes: Tackling water quality. *Journal of Environmental Management* **2021**, *280*, 111680. DOI: 10.1016/j.jenvman.2020.111680
- [62] Reghioua, A.; Barkat, D.; Jawad, A.H.; Abdulhameed, A.S.; Khan, M.R. Synthesis of Schiff's base magnetic crosslinked chitosan-glyoxal/ZnO/Fe₃O₄ nanoparticles for enhanced adsorption of organic dye: Modeling and mechanism study. *Sustainable Chemistry and Pharmacy* **2021**, *20*, 100379. DOI: 10.1016/j.scp.2021.100379
- [63] Saghir, S.; Xiao, Z. Hierarchical mesoporous ZIF-67@LDH for efficient adsorption of aqueous Methyl Orange and Alizarine Red S. *Powder Technology* **2021**, *377*, 453-463. DOI: 10.1016/j.powtec.2020.09.006
- [64] Saghir, S., Xiao, Z. Synthesis of novel Ag@ZIF-67 rhombic dodecahedron for enhanced adsorptive removal of antibiotic and organic dye. *Journal of Molecular Liquids* **2021**, *328*, 115323. DOI: 10.1016/j.molliq.2021.115323
- [65] Shen, T.; Mao, S.; Ding, F.; Han, T.; Gao, M. Selective adsorption of cationic/anionic tritoluene dyes on functionalized amorphous silica: A mechanistic correlation between the precursor, modifier and adsorbate. *Colloids and Surfaces A: Physicochemical and Engineering Aspects* **2021**, *618*, 126435. DOI: 10.1016/j.colsurfa.2021.126435
- [66] Shi, X.; Zu, Y.; Jiang, S.; Sun, F. An anionic indium-organic framework with spirobifluorene-based ligand for selective adsorption of organic dyes. *Inorganic Chemistry* **2021**, *60*, 1571-1578. DOI: 10.1021/acs.inorgchem.0c02962
- [67] Sirajudheen, P.; Karthikeyan, P.; Ramkumar, K.; Nisheetha, P.; Meenakshi, S. Magnetic carbon-biomass from the seeds of *Moringa oleifera*@MnFe₂O₄ composite as an effective and recyclable adsorbent for the removal of organic pollutants from water. *Journal of Molecular Liquids* **2021**, *327*, 114829. DOI: 10.1016/j.molliq.2020.114829
- [68] Sirajudheen, P.; Karthikeyan, P.; Vigneshwaran, S. M. C, B.; Meenakshi, S. Complex interior and surface modified alginate reinforced reduced graphene oxide-hydroxyapatite hybrids: Removal of toxic azo dyes from the aqueous solution. *International Journal of Biological Macromolecules* **2021**, *175*, 361-371. DOI: 10.1016/j.ijbiomac.2021.02.024
- [69] Trinh, T.T.P.N.X.; Nguyet, D.M.; Quan, T.H.; Anh, T.N.M.; Thinh, D.B.; Tai, L.T.; Lan, N.T.; Trinh, D.N.; Dat, N.M.; Nam, H.M.; Phong, M.T.; Hieu, N.H. Preparing three-dimensional graphene aerogels by chemical reducing method: Investigation of synthesis condition and optimization of adsorption capacity of organic dye. *Surfaces and Interfaces* **2021**, *23*, 101023. DOI: 10.1016/j.surfin.2021.101023

- [70] Usman, M.; Ahmed, A.; Yu, B.; Wang, S.; Shen, Y.; Cong, H. Simultaneous adsorption of heavy metals and organic dyes by β -Cyclodextrin-Chitosan based cross-linked adsorbent. *Carbohydrate Polymers* **2021**, *255*, 117486. DOI: 10.1016/j.carbpol.2020.117486
- [71] Vigneshwaran, S.; Sirajudheen, P.; Nikitha, M.; Ramkumar, K.; Meenakshi, S. Facile synthesis of sulfur-doped chitosan/biochar derived from tapioca peel for the removal of organic dyes: Isotherm, kinetics and mechanisms. *Journal of Molecular Liquids* **2021**, *326*, 115303. DOI: 10.1016/j.molliq.2021.115303
- [72] Vigneshwaran, S.; Sirajudheen, P.; Karthikeyan, P.; Meenakshi, S. Fabrication of sulfur-doped biochar derived from tapioca peel waste with superior adsorption performance for the removal of Malachite green and Rhodamine B dyes. *Surfaces and Interfaces* **2021**, *23*, 100920. DOI: 10.1016/j.surfin.2020.100920
- [73] Wang, M.; Guo, Y.; Fu, X.; Cui, H.; Sun, T.; Tang, Y.; Liu, Q. Facile synthesis of novel $\text{Zn}_3(\text{OH})_2\text{V}_2\text{O}_7 \cdot 2\text{H}_2\text{O}$ nanocables with excellent adsorption properties. *Materials Letters* **2021**, *283*, 128710. DOI: 10.1016/j.matlet.2020.128710
- [74] Wang, Q.; Wang, X.; He, H.; Chen, W. Fabrication of hollow LDH nanocages using ZIF-67 template as superb adsorbent for anionic organic pollutant. *Journal of Porous Materials* **2021**, *28*, 471-480. DOI: 10.1007/s10934-020-01007-7
- [75] Wang, X.; Zhang, Y.; Shan, R.; Hu, H. Polydopamine interface encapsulating graphene and immobilizing ultra-small, active Fe_3O_4 nanoparticles for organic dye adsorption. *Ceramics International* **2021**, *47*, 3219-3231. DOI: 10.1016/j.ceramint.2020.09.160
- [76] Wu, J.; Liu, J.; Wen, B.; Li, Y.; Zhou, B.; Wang, Z.; Yang, S.; Zhao, R. Nitrogen-rich covalent triazine frameworks for high-efficient removal of anion dyes and the synergistic adsorption of cationic dyes. *Chemosphere* **2021**, *272*, 129622. DOI: 10.1016/j.chemosphere.2021.129622
- [77] Wu, X.-M.; Liu, L.-X.; Liu, L.; You, Z.-H.; Guo, H.-X.; Chen, Z.-X. Ultrasound assisted synthesis of nanoscale $\text{NH}_2\text{-MIL-53(Fe)}$ for the adsorption of dye. *Jiegou Huaxue* **2021**, *40*, 42-46. DOI: 10.14102/j.cnki.0254-5861.2011-2763
- [78] Xiong, Z.; Wang, Y.; Xie, X.; Li, H.; Yao, C. Synthesis of poly(cyclotriphosphazene-co-3,3'-sulfonyldianilide) microspheres and their adsorption of anionic (congo red) dye. *Heterocycles* **2021**, *102*, 231-244. DOI: 10.3987/COM-20-14366
- [79] Yang, S.; Zhao, F.; Sang, Q.; Zhang, Y.; Chang, L.; Huang, D.; u, B. Investigation of 3-aminopropyltriethoxysilane modifying attapulgit for Congo red removal: Mechanisms and site energy distribution. *Powder Technology* **2021**, *383*, 74-83. DOI: 10.1016/j.powtec.2021.01.046
- [80] Yang, Z.; Liu, X.; Liu, X.; Wu, J.; Zhu, X.; Bai, Z.; Yu, Z. Preparation of β -cyclodextrin/graphene oxide and its adsorption properties for methylene blue. *Colloids and Surfaces B: Biointerfaces* **2021**, *200*, 111605. DOI: 10.1016/j.colsurfb.2021.111605
- [81] Yeamin, M.B.; Islam, M.M.; Chowdhury, A.-N.; Awual, M.R. Efficient encapsulation of toxic dyes from wastewater using several biodegradable natural polymers and their composites. *Journal of Cleaner Production* **2021**, *291*, 125920. DOI: 10.1016/j.jclepro.2021.125920
- [82] Zhan, B.; Liu, Y.; Zhou, W.-T.; Li, S.-Y.; Chen, Z.-B.; Stegmaier, T.; Aliabadi, M.; Han, Z.-W.; Ren, L.-Q. Multifunctional 3D GO/g-C₃N₄/TiO₂ foam for oil-water separation and dye adsorption. *Applied Surface Science* **2021**, *541*, 148638. DOI: 10.1016/j.apsusc.2020.148638
- [83] Zhang, B.; Jin, Y.; Qi, J.; Chen, H.; Chen, G.; Tang, S. Porous carbon materials based on *Physalis alkekengi* L. husk and its application for removal of malachite green. *Environmental Technology and Innovation* **2021**, *21*, 101343. DOI: 10.1016/j.eti.2020.101343
- [84] Zhang, H.-Y.; Liu, L.; Wang, H.-J.; Sun, J.-W. Asymmetrical modification of Keggin polyoxometalates by sextuple Ag-N coordination polymeric chains: Synthesis, structure and selective separation of cationic dyes. *Journal of Solid State Chemistry* **2021**, *296*, 121986. DOI: 10.1016/j.jssc.2021.121986

- [85] Zhang, W.; Yang, X.; Lin, C.; Feng, J.; Wang, H.; Yan, W. Insight into the effect of surfactant modification on the versatile adsorption of titanate-based materials for cationic and anionic contaminants. *Chemosphere* **2021**, 269, 129383. DOI: 10.1016/j.chemosphere.2020.129383
- [86] Zhao, Z.; Bai, C.; An, L.; Zhang, X.; Wang, F.; Huang, Y.; Qu, M.; Yu, Y. Biocompatible porous boron nitride nano/microrods with ultrafast selective adsorption for dyes. *Journal of Environmental Chemical Engineering* **2021**, 9, 104797. DOI: 10.1016/j.jece.2020.104797